

# Stain unmixing in brightfield multiplexed immunohistochemistry

Cédric Wemmert<sup>1</sup>, Juliane M. Krüger<sup>2</sup>, Germain Forestier<sup>3</sup>, Ludovic Sternberger<sup>5</sup>,  
Friedrich Feuerhake<sup>4</sup>, Pierre Gançarski<sup>1</sup>

<sup>1</sup> University of Strasbourg, ICube (UMR 7357 CNRS/Unistra), France

<sup>2</sup> Roche Diagnostics GmbH, Penzberg, Germany

<sup>3</sup> University of Haute-Alsace, MIPS laboratory, France

<sup>4</sup> Hannover Medical School, Germany

<sup>5</sup> Roche Pharma Ltd, Basel, Switzerland

**Abstract**—Automated image analysis of multiplexed brightfield immunohistochemistry assays is a challenging objective. One central task of the analysis is the robust identification of the different stains in the image, called stain unmixing. Stain unmixing strongly depends on the method of image acquisition. Currently available multispectral cameras enable color unmixing of single fields of view (FoV), selected by matter experts (e.g. pathologists). Beyond the individual FoV approach, there is an increasing need to process larger regions or whole histopathological sections (whole slide imaging; WSI). Rapid color deconvolution in WSI is a challenge that is only partially solved. We propose a method based on a multilayer perceptron to compute dye-specific stain layers for chromogenic red and brown labeling in WSI.

**Index Terms**—biomedical imaging, immunohistochemistry, color deconvolution, multilayer perceptron

## I. INTRODUCTION

Immunohistochemistry (IHC) is a widely used diagnostic tool to detect proteins in tissue sections by the use of specific antibodies. The proteins are visualized using a reporter enzyme that binds to the antibody and a chromogenic, fluorogenic or chemiluminescent substrate which can be visualized. In comparison to other techniques that detect proteins in tissue homogenates (e.g. Western blot, Elisa) and hence lose the spatial dimension, IHC retains the tissue architecture and can be used to determine the distribution and localization of proteins.

Multiplexed immunohistochemistry refers to the detection of several proteins in a single tissue section. Analyzing several proteins at once is for instance required for the simultaneous assessment of several hallmarks of cancer, for the detection of subpopulations of immune cells, subcategorizing vessels, or analyzing multiple pathways at once [1], [2], [3], [4], [5]. In case of chromogenic detection of the proteins, a variety of substrates is available generating different colors for each protein. In Figure 1, the color properties of two commonly used chromogenic substrates, 3,3-diaminobenzidine tetrahydrochloride (DAB) and Permanent Red (PRD), and the nuclear counterstain hematoxylin (HLN) are illustrated. In addition, the co-occurrence of PRD and DAB is demonstrated using an artificial double staining to detect a single antigen with two substrates.

Routinely, the stained glass slides are read by a pathologist. In addition, digital pathology has gained increased importance

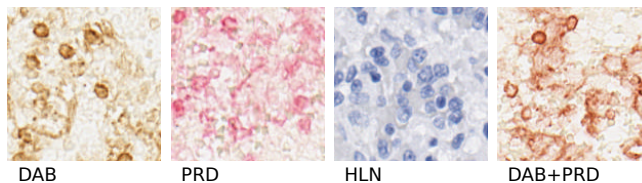


Fig. 1. Illustration of two chromogenic substrates DAB (brown) and PRD (pink), the counterstaining HLN (blue) and the co-localization of DAB and PRD (brown-red).

in recent years [6], [7]. Digital pathology refers to the automated or semi-automated image analysis of digitalized glass slides or FoVs of glass slides. The automated image analysis is especially important for supplying image data that is difficult to capture by the pathologist. Analyzing multiplexed immunohistochemistry slides requires the differentiation of the used stains, called stain unmixing.

The stain unmixing process differs whether the image acquisition is performed using: (I) a CCD color camera mounted on a microscope or a scanner and allowing the acquisition of an RGB image of selected FoVs or the whole slide, respectively; or (II) a multispectral imaging (MSI) system providing a wide spectral range for each pixel<sup>1</sup> for selected FoVs of the slide.

MSI provides richer information than RGB acquisition, and the software allows an automated unmixing of the stains. However, MSI is time consuming and limited to single FoVs, introducing a bias by the observer who selects representative fields of interest [8]. Being able to unmix the different stainings robustly from an RGB scan would circumvent this problem and allow the analysis in WSI.

In this paper, we propose a method which estimates the contribution of the different dyes for each pixel of an RGB image, thereby enabling the analysis of an entire slide. The challenge is to find a way to determine the function needed to compute the staining contribution of the pixels from the RGB image.

## II. RELATED WORK

The colorimetric 3D RGB space of the pixels from the single- and double-stained images of Figure 1 is presented in

<sup>1</sup>from 420-720nm in 10 or 20nm steps for the PerkinElmer Nuance FX™ for example

Figure 2. Whereas the single-stained pixels (HLN, PRD and DAB) seem to be separable in this space, the double-stained pixels (DAB+PRD in our example) that are located between the two clusters of single-stained pixels are difficult to identify.

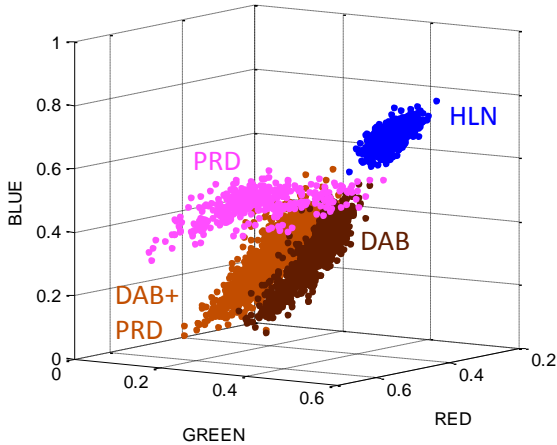


Fig. 2. Projection of the different stains shown in Figure 1 plotted in RGB space.

Different work has been done to provide efficient classification methods of the stains in the RGB color space. These methods are mainly based on linear or planar projection to separate the individual stains [9], [10]. Unfortunately, classifying each pixel according to the 3D domains of the different stains is time-consuming and complex because it requires the manual sampling of pure single-stained and double-stained pixels.

Another approach to enhance the separability of the different stainings consists of making a colorspace conversion or transformation. For example, Laak *et al.* [11] proposed a new model derived from the traditional Hue-Saturation-Intensity (HSI). The idea is to apply the RGB to HSI transform to optical densities (OD) for the individual RGB channels instead of intensities. As the chromatic component of the HSD model is independent of the amount of stain, the obtained colorimetric space better discriminates between the absorption characteristics of the different stains.

Ruifrok *et al.* [12] developed a color deconvolution method for up to three stains that works in the OD converted RGB colorspace. The user has to determine the OD values of the pure stains. The assumption is that each pixel in the image can be represented by a linear combination of the different stains. Hence, solving a system of linear equations computes the amount of each stain present in each pixel.

More recently, Rabinovitch *et al.* [13] proposed a fully automated color decomposition process to determine the amount of each dye in the sample. Unfortunately, this method can only be applied on a multispectral stack of images, and not on traditional brightfield RGB images.

The approach presented in this paper differs from the ones described above. We propose to build a transformation function that directly projects the pixels from the RGB into the desired 3D space composed of the different stains here:

HLN, DAB and PRD. As this transformation function is nonlinear, we decided to use a multilayer perceptron to learn and represent this transformation. The unmixed staining layers generated by the multispectral acquisition and analysis system is taken as a ground truth to learn the transformation.

### III. DECONVOLUTION METHOD

Our approach is based on three steps: (I) Colorimetric homogenization of the pseudo-RGB image generated with MSI and the RGB image acquired with a CCD camera (scanner or microscope); (II) Training of the multilayer perceptron; (III) Application of the learned transformation on all RGB images.

After these steps, segmentation algorithms can be used to detect objects (*e.g.* cells, subcellular compartments) in the image.

#### A. Colorimetric homogenization

Due to the differences in hardware (MSI with liquid tunable filters to sample at wavelengths in the visible range versus a three filter RGB CCD chip in case of a microscope or scanner), the RGB images of the two acquisition methods differ significantly (see leftmost column of Figure 4). A histogram specification algorithm is applied in order to make these RGB images comparable.

Histogram specification, or histogram matching, is a basic histogram modeling technique that transforms one histogram into another by remapping the pixel values to control the relative frequency of their occurrence. It uses a simple monotonic, nonlinear mapping to re-assign the intensity values of pixels in the input image such that the target and output image histograms look alike [14]. The histogram specification is applied in both colorimetric spaces RGB and Hue-Saturation-Value (HSV).

#### B. Multi-layer perceptron training

The main challenge poses the definition of a direct transformation function (Eq. (1)) from the RGB space to another 3D space, based on the stains of the image.

$$\begin{cases} t : \mathbb{R}^3 \rightarrow \mathbb{R}^3 \\ t(r, g, b) = (h, d, p) \end{cases} \quad (1)$$

As this function is nonlinear, we decided to use a multilayer perceptron to approximate it.

A perceptron or an artificial neuron, as introduced by McCulloch and Pitts [15], is the mathematical model of a neuronal cell and the basic building block of an artificial neural network. The perceptron architecture consists of a set of  $n$  inputs ( $x_i$ ), each one associated to a weight ( $w_i$ ) and an activation function ( $f_i$ ). Perceptrons can be organized to form a layer in which all perceptrons are linked to the same inputs but have distinct outputs. This kind of network is called a perceptron network. It is well-known that perceptron networks perform well if the pattern to be recognized is linearly separable; however, they should not be used to solve complex classification problems involving non-linearly separable patterns. In case of non-linearly separable patterns, a multilayer perceptron network (MLP) can be used instead [16].

An MLP consists of multiple layers of artificial neurons (an input layer, one or more intermediate or hidden layers, and an output layer) in a directed graph, with each layer fully connected to the next one. Since this artificial neuronal network topology can solve classification problems involving non-linearly separable patterns, it can be used as a universal function generator. MLPs have two distinct phases: training and execution. For the training, the most widely used algorithm is the backpropagation [17].

In our case, the structure of the MLP is composed of (as shown on Figure 3): one input layer of three input neurons (one for each color red, green and blue); two hidden layers of six neurons each; one output layer of three output neurons (one for each calculated channel: HLN, DAB and PRD).

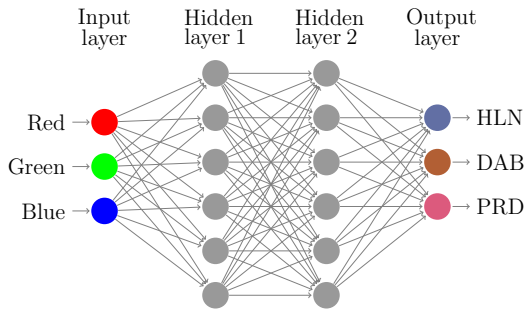


Fig. 3. Structure of the MLP used to learn the colorimetric space-transformation.

The activation function used for each neuron is a standard sigmoid function, expressed in equation (2), with  $\lambda = 2$ .

$$f_i(x) = \frac{1}{1 + e^{-\lambda x}} \quad (2)$$

The samples to train the MLP were chosen in the multispectral image to represent areas with single- and double-stained pixels.

## IV. EXPERIMENTS AND RESULTS

### A. Dataset presentation

To validate our approach, we used 33 formalin-fixed paraffin-embedded breast cancer samples obtained from Indivumed®, Hamburg, Germany. Manual immunohistochemistry staining was performed for CD8 (Figure 1, Ventana) or CD3/Perforin (Figure 4, see [3]) and antibody binding was visualized using 3,3-diaminobenzidine tetrahydrochloride (DAB, Dako, Hamburg, Germany) and Permanent Red (PRD, Zytomed, Berlin, Germany). Cell nuclei were counterstained with hematoxylin before mounting. Single staining without hematoxylin counterstain was performed for selected cases to generate pure DAB and PRD spectra for multispectral analysis.

**Image acquisition** - Conventional brightfield images of duplex IHC staining were taken using a Leica DM6000B equipped with a Leica DFC480 digital camera, using the LASv3.7 software. Whole slide scans were acquired using the Aperio ScanScope XT. Multispectral imaging of selected cases (ground truth) was performed with the Nuance FX

	MLP	Ruifrok	Laak
HLN	0.098 ± 0.065	0.219 ± 0.099	0.315 ± 0.235
DAB	0.060 ± 0.064	0.171 ± 0.105	0.048 ± 0.289
PRD	0.013 ± 0.087	0.013 ± 0.206	0.019 ± 0.304
$\Sigma$	0.171	0.403	0.381

TABLE I  
MEANS AND STANDARD DEVIATIONS OF THE DIFFERENCE BETWEEN EACH CHANNEL (HLN, DAB, PRD) AND THE CORRESPONDING CHANNEL ACQUIRED WITH THE NUANCE CAMERA.

system (CRi/Caliper, Hopkinton, MA, USA) following the manufacturers instructions.

### B. Comparison with existing methods

To evaluate the performance of our method, we present in Figure 4 a visual comparison of the three channels calculated by the deconvolution methods presented by van der Laak [11] (custom implementation in Matlab), Ruifrok [12] (Cellprofiler implementation [18]) and our MLP method.

The first line corresponds to the MSI unmixing results, considered here as the ground truth. Obviously, the approach of van der Laak [11] is least suited to the specific problem of color deconvolution addressed in our work. Specifically, the signal provided in the HLN channel is too strong and largely unspecific. Thus, it cannot be used to extract cell nuclei. In addition, the PRD channel is weak and some pixels are missed. The deconvolution method of Ruifrok [12] provides very good results for both the HLN and PRD channel. Unfortunately, problems appear in the DAB channel, that not only shows DAB-positive but also PRD-positive pixels (marked by the yellow arrows in Fig. 4).

Visually, the results provided by the MLP learning method resulted in the best match with our ground truth of MSI. Of note, the HLN channel shows weaker signals, but this did not impact the overall performance of the algorithm with regard to the downstream image processing for our specific biological question.

These observations are reinforced by values obtained by calculating the difference between each generated channel and our ground truth (see Table I).

## V. CONCLUSION

In this paper, we presented an improved way to automatically deconvolve the RGB image of a IHC stained histopathological slide into different dye absorption channels. The method is based on the training of an MLP that learns the transformation function from samples selected in a multispectral *ground truth* image. As the training is done once for a set of similar images, and only on a few samples, the method can easily be applied to WSI.

## REFERENCES

- [1] D. Hanahan and R. Weinberg, "The hallmarks of cancer," *Cell*, vol. 100, no. 1, pp. 57–70, 2000.
- [2] —, "Hallmarks of cancer: the next generation," *Cell*, vol. 144, no. 5, pp. 646–674, 2011.

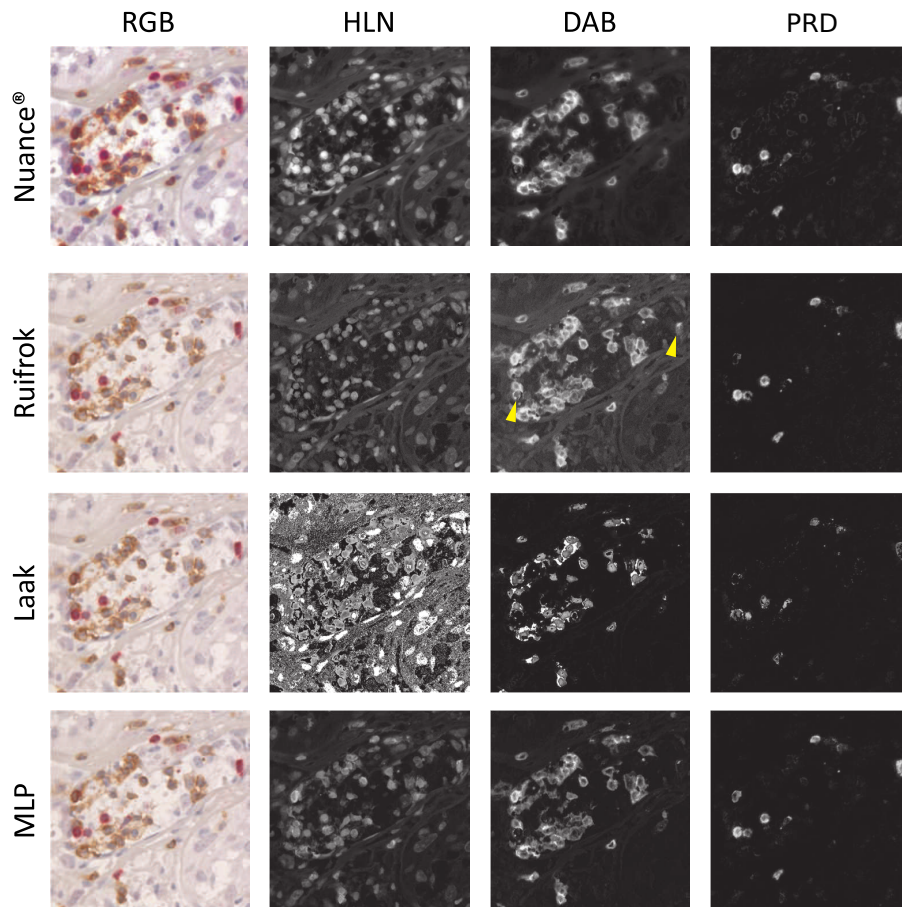


Fig. 4. Comparison of the results obtained with different deconvolution methods: first line corresponds to the Nuance multispectral acquisition (considered as the ground truth here), next lines are presenting the results of the Ruifrok method [12], the Laak method [11] and our MLP learning method, respectively.

- [3] J. M. Krüger, C. Wemmer, L. Sternberger, C. Bonnas, G. Dietmann, P. Gançarski, and F. Feuerhake, "Combat or surveillance? evaluation of the heterogeneous inflammatory breast cancer microenvironment." *J Pathol*, 2012.
- [4] B. L. Falcon, J. Stewart, S. Ezell, J. Hanson, J. Wijsman, X. Ye, E. Westin, G. Donoho, K. Credille, and M. T. Uhlik, "High-content multiplexed tissue imaging and quantification for cancer drug discovery." *Drug Discov Today*, 2012.
- [5] C. Bonnas, K. Specht, O. Spleiss, S. Froehner, G. Dietmann, J. M. Krüger, S. Arbogast, and F. Feuerhake, "Effects of cold ischemia and inflammatory tumor microenvironment on detection of pi3k/akt and mapk pathway activation patterns in clinical cancer samples." *Int J Cancer*, vol. 131, no. 7, pp. 1621–32, 2012.
- [6] S. Al-Janabi, A. Huisman, and P. J. Van Diest, "Digital pathology: current status and future perspectives." *Histopathology*, vol. 61, no. 1, pp. 1–9, 2012.
- [7] L. Cooper, A. Carter, A. Farris, F. Wang, J. Kong, D. Gutman, P. Widener, T. Pan, S. Cholleti, A. Sharma, T. Kurc, D. Brat, and J. Saltz, "Digital pathology: Data-intensive frontier in medical imaging." *Proceedings of the IEEE*, vol. 100, no. 4, pp. 991–1003, april 2012.
- [8] R. M. Levenson, "Spectral imaging perspective on cytomics," *Cytometry Part A*, vol. 69, no. 7, pp. 592–600, 2006.
- [9] A. Sarabi and J. K. Aggarwal, "Segmentation of chromatic images," *Pattern Recognition*, vol. 13, no. 6, pp. 417–427, 1981.
- [10] C. MacAulay, H. Tezcan, and B. Palcic, "Adaptive color basis transformation. an aid in image segmentation." *Anal Quant Cytol Histol*, vol. 11, no. 1, pp. 53–8, 1989.
- [11] J. A. van Der Laak, M. M. Pahlplatz, A. G. Hanselaar, and P. C. de Wilde, "Hue-saturation-density (hsd) model for stain recognition in digital images from transmitted light microscopy." *Cytometry*, vol. 39, no. 4, pp. 275–84, 2000.
- [12] A. C. Ruifrok and D. A. Johnston, "Quantification of histochemical staining by color deconvolution." *Anal Quant Cytol Histol*, vol. 23, no. 4, pp. 291–299, Aug. 2001.
- [13] A. Rabinovich, S. Agarwal, C. Laris, J. H. Price, and S. Belongie, "Unsupervised color decomposition of histologically stained tissue samples." in *NIPS*, S. Thrun, L. K. Saul, and B. Schölkopf, Eds. MIT Press, 2003.
- [14] R. C. Gonzalez and R. E. Woods, *Digital Image Processing*, 2nd ed. Boston, MA, USA: Addison-Wesley Longman Publishing Co., Inc., 2001.
- [15] W. S. McCulloch and W. Pitts, "A logical calculus of the ideas immanent in nervous activity," *Bulletin of Mathematical Biophysics*, vol. 5, pp. 115–133, 1943.
- [16] F. Rosenblatt, "The perceptron: a probabilistic model for information storage and organization in the brain." *Psychological review*, vol. 65, no. 6, pp. 386–408, Nov. 1958.
- [17] D. E. Rumelhart, G. E. Hinton, and R. J. Williams, "Neurocomputing: foundations of research," J. A. Anderson and E. Rosenfeld, Eds. Cambridge, MA, USA: MIT Press, 1988, ch. Learning internal representations by error propagation, pp. 673–695.
- [18] M. R. Lamprecht, D. M. Sabatini, and A. E. Carpenter, "Cellprofiler: free, versatile software for automated biological image analysis," *Biotechniques*, vol. 42, no. 1, pp. 71–75, 2007.